

DMD 28043

*In vitro* Inhibition of Multiple Cytochrome P450 Isoforms by  
Xanthone Derivatives from Mangosteen Extract

Robert S. Foti, Josh T. Pearson, Dan A. Rock, Jan L. Wahlstrom  
and Larry C. Wienkers

Pharmacokinetics and Drug Metabolism, Amgen, Inc.  
Seattle, WA 98119  
(RSF, JTP, DAR, JLW, LCW)

DMD 28043

**Running title:**

**Inhibition of Cytochrome P450 *In Vitro* by Xanthone Derivatives**

**Corresponding author:**

Robert S. Foti

Amgen, Inc  
Pharmacokinetics and Drug Metabolism  
1201 Amgen Court West  
Mail Stop AW2/D2751  
Seattle, WA 98119  
(206)265-7164  
rfoti@amgen.com

**Manuscript metrics:**

text pages 20

tables 2

figures 5

references 37

words in the abstract 142

words in the introduction 503

words in the results and discussion 2293 (1270 Results / 1023 Discussion)

**Abbreviations:** cytochrome P450, CYP; liquid chromatography – tandem mass spectrometry, LC-MS/MS; US Food and Drug Administration, FDA;

DMD 28043

## Abstract

Mangosteen is a xanthone-containing fruit found in Southeast Asia whose health claims include maintaining healthy immune and gastrointestinal systems to slowing the progression of tumor growth and neurodegenerative diseases. Previous studies have identified multiple xanthones in the pericarp of the mangosteen fruit. The aim of the current study was to assess the drug inhibition potential of mangosteen *in vitro* as well as the cytochrome P450 (CYP) enzymes responsible for the metabolism of its individual components. The various xanthone derivatives were found to be both substrates and inhibitors for multiple CYP isoforms. Aqueous extracts of the mangosteen pericarp were analyzed for xanthone content as well as inhibition potency. Finally, *in vivo* plasma concentrations of  $\alpha$ -mangostin, the most abundant xanthone derivative found in mangosteen, were predicted using SimCYP and found to be well above their respective *in vitro*  $K_i$  values for CYP2C8 and CYP2C9.

DMD 28043

## Introduction

The use of alternative or herbal remedies, both as single therapies and in combination, has increased steadily in recent years (Craig, 1999; Ritchie, 2007). Current estimates place the sales of herbal remedies and nutraceuticals at well over \$4 billion dollars in the United States alone (Blumenthal et al., 2006). In addition to the sales of herbal therapies, the number of reports of adverse events related to the use of such products has also risen (Skalli et al., 2007). Not surprisingly, the research community as a whole has placed a greater emphasis on the characterization and safety profiles of widely used herbal therapies both in the United States and around the world (Foti and Wahlstrom, 2008).

The incidence of potential cytochrome P450 (CYP) mediated drug inhibition from herbal therapies has been noted for such popular remedies as St. John's wort, echinacea, ginseng, garlic and saw palmetto (Obach, 2000; Modarai et al., 2007; Chang et al., 2002; He and Edeki, 2004; Liu et al., 2006; Foster et al., 2001; Yale and Glurich, 2005). Various herbal constituents have also been shown to induce CYP activity *in vitro*. Herbal CYP inducers include ginkgo (CYP2C19), ginseng (CYP2C9), echinacea (CYP3A4) and St. John's wort (CYP1A2, CYP2C9, CYP2C19, CYP2E1 and CYP3A4) (Tirona and Bailey, 2006). While clinical examples of such interactions lag behind the *in vitro* literature, examples such as garlic (CYP2E1) and goldenseal (CYP2D6 and CYP3A) have been observed (Gurley et al., 2005a; Markowitz et al., 2003; Gurley et al., 2005b).

Mangosteen is a tropical fruit that is indigenous to Southeast Asia but can be found in most tropical countries (Ji et al., 2007). The major therapeutic

DMD 28043

benefits come from the pericarp of the fruit, which has been shown to contain numerous biologically active compounds such as xanthenes, terpenes, anthocyanins, tannins, phenols and multiple vitamins (Kosem et al., 2007). Mangosteen has historically been used to treat abdominal pain, skin infections and diarrhea, and more recently has been proposed as a homeopathic therapy in the treatment of Parkinson's disease (Jung et al., 2006). Xanthenes from mangosteen have also been shown to be inhibitors of CYP19 (aromatase), potentially resulting in the anti-tumor properties of the compounds (Balunas et al., 2008).

The aim of this study was to characterize the metabolism and drug interaction potential of six xanthone derivatives ( $\alpha$ -mangostin,  $\beta$ -mangostin, gartanin, 3-isomangostin, 8-desoxygartanin and 9-hydroxycalabaxanthone) that are found in the pericarp of the mangosteen fruit. Xanthone content from commercially available mangosteen products was measured following extraction with either water or acetone. Inhibition against 8 CYP isoforms was assessed for each of the six analogs as well as an aqueous extraction of the whole pericarp suspension. Reaction phenotyping experiments were performed on the analogs to determine the CYP isoforms responsible for their metabolism. Finally, *in vivo* plasma concentrations of  $\alpha$ -mangostin were modeled using SimCYP and compared to *in vitro* inhibition data. Results demonstrate that mangosteen and its individual components have the ability to inhibit CYP activity and as such, care should be taken when using mangosteen products in conjunction with traditional therapeutics.

DMD 28043

## Materials and Methods

*Materials.* Pooled human liver microsomes and recombinant CYP Supersomes® were obtained from Xenotech LLC (Lenexa, KS) and BD Biosciences (San Jose, CA), respectively.  $\alpha$ -Mangostin,  $\beta$ -mangostin, gartanin, 3-isomangostin, 8-desoxygartanin and 9-hydroxycalabaxanthone were obtained from ChromaDex (Irvine, CA). Phenacetin, acetaminophen, bupropion, diclofenac, dextromethorphan, dextrophan, 6 $\beta$ -hydroxytestosterone, midazolam, and 1'-hydroxymidazolam were purchased from Sigma Chemical Co. (St. Louis, MO). Chlorzoxazone and paclitaxel were from MP Biomedicals (Solon, OH). (S)-mephenytoin was obtained from Biomol International (Plymouth Meeting, PA). 6-hydroxypaclitaxel and reduced  $\beta$ -NADPH were purchased from Calbiochem (San Diego, CA). 4'-Hydroxy-(S)-mephenytoin, 4'-hydroxydiclofenac and 6-hydroxychlorzoxazone were purchased from BD Biosciences (San Jose, CA). Testosterone was purchased from Steraloids (Newport, RI).

*Component Analysis of Mangosteen Whole Extract.* A whole extract of mangosteen pericarp from wild harvested mangosteen labeled to contain no additional ingredients (GenesisToday™; Austin, TX) was purchased from a local pharmacy and assayed for the presence of inhibitory xanthone derivatives. The pericarp sample was extracted using either acetone or water in a manner similar to that described in Ji, et al (2007). In brief, the pericarp extract was shaken to ensure homogeneity and added to 2 volumes (v/v) of acetone or water. The sample was then vortexed for 20 minutes and centrifuged for 15 minutes at 3000

DMD 28043

rpm. The resulting supernatant was concentrated under a gentle stream of N<sub>2</sub> at 30°C prior to analysis by LC-MS/MS.

*IC<sub>50</sub> Determination.* The incubation time and protein concentrations used were within the linear range for each respective CYP probe reaction. In addition, no more than 15 – 20% turnover of the xanthone derivatives occurred over 30 minutes in human liver microsomes. Probe substrates were run at their estimated *K<sub>m</sub>* values (phenacetin O-dealkylation, 30 μM; bupropion 1-hydroxylation, 80 μM; paclitaxel 6α-hydroxylation, 7 μM; diclofenac 4-hydroxylation, 5 μM; (S)-mephenytoin 4'-hydroxylation, 20 μM; dextromethorphan O-demethylation, 5 μM; chlorzoxazone 6-hydroxylation 75 μM; midazolam 1'-hydroxylation, 1.5 μM; testosterone 6β-hydroxylation, 50 μM;) and all incubations contained less than 1% organic solvent (v/v). Incubation conditions (run in duplicate) included pooled human liver microsomes (0.1 mg/mL, final concentration), 3 mM MgCl<sub>2</sub>, 100 mM potassium phosphate buffer (pH 7.4) and 1 mM NADPH in a final volume of 100 μL. Final inhibitor concentrations ranged from 0 – 20 μM for the mangostin xanthone derivatives and from 0 – 1 g/mL of the whole mangosteen extract. All incubations were conducted at 37°C, pre-incubated for 3 minutes prior to addition of NADPH, and quenched with 2 volumes of ice cold acetonitrile containing 0.1 μM tolbutamide as internal standard after 20 minutes (5 minutes for incubations where midazolam was used as the probe substrate). Samples were then vortexed and centrifuged (3000 rpm, 10 minutes) prior to LC-MS/MS analysis.

*K<sub>i</sub> Determination.* For compounds whose *IC*<sub>50</sub> value was determined to be less than 3  $\mu$ M for a given CYP isoform, a *K<sub>i</sub>* assessment was made in pooled human liver microsomes. A matrix of four probe substrate concentrations (0.5x *K<sub>m</sub>*, *K<sub>m</sub>*, 2x *K<sub>m</sub>* and 4x *K<sub>m</sub>*) and five inhibitor concentrations (spanning a 10-fold range around the estimated *K<sub>i</sub>*) was used to determine a *K<sub>i</sub>* value for each xanthone derivative. Reaction conditions and sample preparation procedures were identical to those described above for the *IC*<sub>50</sub> determinations. All *K<sub>i</sub>* determinations were run in duplicate.

*Inhibition of CYP Reductase.* To test for the possibility that the xanthone derivatives from mangosteen were also inhibitors of CYP reductase, a CYP reductase activity kit was obtained and used according to the supplier's instructions (Sigma, St. Louis, MO). CYP reductase activity (measured as change in absorbance at 550 nm) in the presence of each xanthone (10  $\mu$ M) was measured and compared to activity in negative (solvent only) and positive (diphenyleneiodinium) inhibitor controls.

*Statistical Analysis.* Standard curves and mass spectrometry data were fit using Analyst (version 1.4; Applied Biosystems, Foster City, CA). In general, standard curves were weighted using 1/x. Analysis of *IC*<sub>50</sub> and *K<sub>i</sub>* data was performed using Graphpad Prism (version 4.01; Graphpad Software Inc., San Diego, CA). *IC*<sub>50</sub> data was fit using a sigmoidal dose-response model (Equation 1), while *K<sub>i</sub>*



DMD 28043

data was applied to either a competitive (Equation 2) or linear-mixed (Equation 3) model after visual inspection of the Dixon ( $[I]$  vs  $1/v$ ) and Lineweaver-Burke ( $1/[S]$  vs  $1/v$ ) plots. For the equations below,  $[I]$  is the concentration of inhibitor in the system,  $K_m$  is equal to half the substrate concentration at maximal reaction velocity,  $K_i$  is the dissociation constant for the enzyme-inhibitor complex and  $K_i'$  is the dissociation constant for the enzyme-substrate-inhibitor complex. Note that for equation 2 and 3,  $K_m$ ,  $K_i$ ,  $K_i'$  and  $V_{max}$  were treated as global parameters.

$$(1) \quad \% activity = \min + \frac{(\max - \min)}{(1 + 10^{(\log[I] - \log IC50)})}$$

$$(2) \quad v = \frac{V_{max} \bullet [S]}{K_m (1 + \frac{[I]}{K_i}) + [S]}$$

$$(3) \quad v = \frac{V_{max} \bullet [S]}{K_m (1 + \frac{[I]}{K_i}) + [S](1 + \frac{[I]}{K_i'})}$$

*Assessment of Time-Dependent Inhibition.* All six xanthone derivatives were screened for their time-dependent inhibition potential against CYP1A2, CYP2B6, CYP2C8, CYP2C9, CYP2C19, CYP2D6 and CYP3A4 in pooled human liver microsomes. Primary incubations consisted of human liver microsomes (1 mg/mL, final concentration), 3 mM MgCl<sub>2</sub>, an individual xanthone compound (10 μM, final concentration) and 100 mM potassium phosphate buffer. Incubations

DMD 28043

were pre-incubated at 37°C for 3 minutes prior to the addition of 1 mM NADPH (final concentration). At various time points (0, 5, 15 and 30 minutes), a 10 µL aliquot of the primary incubation was added to a secondary incubation containing 3 mM MgCl<sub>2</sub>, a selective probe substrate (final concentration = 5x  $K_m$ ) and 1 mM NADPH in 100 mM potassium phosphate buffer (pH 7.4; final volume = 200 µL). Secondary incubations were terminated after 20 minutes (5 minutes for midazolam) with 2 volumes (v/v) of ice cold acetonitrile containing 0.1 µM tolbutamide as internal standard. Incubations were run in duplicate and samples handled in a similar fashion as described for the  $IC_{50}$  and  $K_i$  determinations prior to LC-MS/MS analysis. Control experiments were run to ensure linearity of metabolite formation over the entire course of the incubation (data not shown).

*Reaction Phenotyping.* In order to determine the CYP isoforms responsible for the metabolism of the xanthone analogs, reaction phenotyping was carried out using recombinantly cDNA-expressed CYP enzymes. Briefly, each analog (1 µM, final concentration) was incubated with 10 pmol of CYP1A2, CYP2B6, CYP2C8, CYP2C9, CYP2C19, CYP2D6, CYP2E1 and CYP3A4 in 100 mM potassium phosphate buffer (pH 7.4; final volume = 100 µL) containing 3 mM MgCl<sub>2</sub>. Reactions were incubated at 37°C for 3 minutes prior to the addition of 1 mM NADPH (final concentration) to initiate the reaction. Reactions were terminated with the addition of 2 volumes (v/v) ice cold acetonitrile containing 0.1 µM tolbutamide as internal standard after 0, 5, 10, 15, 30 and 45 minutes. Samples

DMD 28043

were subsequently vortexed and centrifuged (3000 rpm, 10 minutes) prior to LC-MS/MS analysis.

*Liquid Chromatography / Mass Spectrometry.* All sample analysis procedures were conducted using LC-tandem mass spectrometry (LC-MS/MS). In brief, the LC-MS/MS system used for all experiments was comprised of an Applied Biosystems 4000 Q-Trap equipped with an electrospray ionization source (Applied Biosystems, Foster City, CA). The MS/MS system was coupled to two LC-20AD pumps with an in-line CBM-20A controller and DGU-20A<sub>5</sub> solvent degasser (Shimadzu, Columbia, MD) and a LEAP CTC HTS PAL autosampler equipped with a dual-solvent self-washing system (CTC Analytics, Carrboro, NC). An injection volume of 20  $\mu$ L was used for all analyses.

For samples from the  $IC_{50}$ ,  $K_i$ , time-dependent inhibition or reaction phenotyping experiments, HPLC separation was achieved using a Gemini C18 2.0 x 30 mm 5  $\mu$ m column (Phenomenex, Torrance, CA). A rapid gradient elution (flow rate = 500  $\mu$ L/min) was carried out using a mobile phase system consisting of (A) 5 mM ammonium formate with 0.1% formic acid and (B) acetonitrile with 0.1% formic acid. HPLC flow was diverted from the MS/MS system for the first 20 seconds to remove any non-volatile salts. Generic MS parameters included the curtain gas (10 arbitrary units), CAD gas (medium), ionspray voltage (4500 V), source temperature (450  $^{\circ}$ C) and ion source gas 1 and gas 2 (40 arbitrary units, each). Interface heaters were kept on for all analytes. Probe substrate mass

DMD 28043

transitions were identical to previously published methods (Walsky and Obach, 2004).

HPLC separation of the xanthone derivatives from the whole mangosteen extract was performed on a Luna C18 2.0 x 150 mm 5 $\mu$ m column (Phenomenex, Torrance, CA). A mobile phase system of (A) water/isopropanol (80/20) with 0.1% formic acid and (B) acetonitrile/isopropanol (80/20) with 0.1% formic acid was used with the following gradient: 50% B isocratic for 5 minutes, 50 to 85% B from 5 to 50 minutes, 85 – 100% B from 50 to 55 minutes, 100 – 50% B from 55 to 56 minutes and finally 50% B isocratic from 56 to 60 minutes (flow rate = 200  $\mu$ L / min). A full scan (100 to 800 amu) was initially run to identify potential xanthone derivatives from the acetone extract. In addition, multiple-reaction monitoring (MRM) methods were used to confirm the identity of the xanthone analogs. MRM transitions for the xanthone compounds were 411.2 / 355.1 ( $\alpha$ -mangostin), 425.1 / 369.1 ( $\beta$ -mangostin), 397.2 / 285.0 (gartanin), 411.1 / 355.2 (3-isomangostin), 381.2 / 325.2 (8-desoxygartanin) and 409.1 / 353.1 (9-hydroxycalabaxanthone). Further characterization of the peaks in the whole extract was obtained by comparing observed MRM's and retention times to those of neat chemical standards.

*Prediction of In Vivo Plasma Concentrations and Drug Interactions.* Human plasma concentrations of  $\alpha$ -mangostin were projected for 6.5 or 75 mg b.i.d. doses of mangosteen using SimCYP (Version 8.01). Dosing levels were selected from a range of reported or observed  $\alpha$ -mangostin concentrations in

DMD 28043

multiple mangosteen products. Molecular weight (410.2 amu), clogP (4.64), calculated pKa (3.76), fraction unbound in plasma (0.05, predicted) and the intrinsic clearance from human hepatocytes (21.7 mL/min/kg; in-house determination utilizing  $1.0 \times 10^6$  cryopreserved hepatocytes / mL and a substrate concentration of 1  $\mu$ M) were input into SimCYP. The remaining physiological and ADME parameters were predicted from SimCYP on the basis of the physicochemical data input for  $\alpha$ -mangostin using a one compartment distribution model (absorption rate constant =  $3.55 \text{ hr}^{-1}$ ; volume of distribution = 0.24 L/kg). The pharmacokinetic simulation was designed to represent 100 healthy volunteers ranging in age from 18 to 65 and divided into 10 trials of 10 subjects each. The dosing interval between each dose was 12 hours. Female subjects represented approximately 34% of the simulated population. In order to account for potential differences in absorption profiles of different mangosteen products, predicted plasma concentrations were plotted for the 75 mg dose at a  $f_a$  (fraction absorbed) of 1, 0.75, 0.5 and 0.25.

To assess drug interaction potential *in vivo*, SimCYP was used to model the *in vivo* drug interaction between  $\alpha$ -mangostin and rosiglitazone, a common substrate cleared by CYP2C8 and CYP2C9. Physicochemical properties and dosing regimen for rosiglitazone were taken directly from SimCYP default values for this compound. All input parameters for  $\alpha$ -mangostin and population characteristics for the drug interaction trials were identical to those described above for predicting *in vivo* plasma concentrations.

## RESULTS

Mangosteen, a plant species found primarily in Southeast Asia, has been receiving an increased amount of attention due to its use as an antioxidant and potential anti-Parkinson's therapy. While the pericarp of the mangosteen fruit has been shown to contain phytochemically active substances such as tannins, terpenes, phenolic compounds and vitamins B1, B2 and C, we have focused on the xanthone component of mangosteen as a potential source of herb-drug interactions *in vitro*. Mangosteen has been shown to contain multiple xanthone derivatives, including  $\alpha$ -mangostin,  $\beta$ -mangostin, gartanin, 3-isomangostin, 8-desoxygartanin and 9-hydroxycalabaxanthone (Figure 1). Multiple xanthenes, including the six mentioned above, were identified in various mangosteen extracts. The whole extracts as well as the individual compounds were assessed for their potential to inhibit CYP activity in either a reversible or time-dependent fashion. The contribution of various CYP isoforms to the metabolism of the xanthone derivative was also assessed. Finally, plasma concentrations of  $\alpha$ -mangostin following multiple doses of mangosteen extract were estimated and compared to *in vitro* inhibition values.

Acetone and aqueous extracts of whole mangostin pericarp were examined for xanthone content as well as drug-interaction potential. All of the six xanthenes mentioned above were identified by LC-MS/MS. In addition, five additional peaks with fragmentation properties similar to the other xanthenes were identified in both extracts (Figure 2). Xanthone derivatives were characterized by comparing retention times to those of known standards as well

DMD 28043

as by molecular weights and mass fragmentation patterns. When compared to standard curves of neat chemical standards, the approximate concentration of each xanthone in the aqueous extract was as follows:  $\alpha$ -mangostin,  $489.0 \pm 36 \mu\text{M}$  (6.01 mg / dose);  $\beta$ -mangostin,  $21.2 \pm 1.4 \mu\text{M}$  (0.27 mg / dose); gartanin,  $22.5 \pm 0.5 \mu\text{M}$  (0.26 mg / dose); 3-isomangostin,  $22.0 \pm 1.7 \mu\text{M}$  (0.28 mg / dose); 8-desoxygartanin,  $48.4 \pm 7.7 \mu\text{M}$  (0.55 mg / dose); 9-hydroxycalabaxanthone,  $189.3 \pm 9.3 \mu\text{M}$  (2.32 mg / dose). Of the additional peaks observed in the chromatogram, the peaks at 5.1 minutes ( $M+H = 411.2$ ) and 16.2 minutes ( $M+H = 397.2$ ) were also observed as potential impurities in the 3-isomangostin chemical standard (data not shown). It is possible that the peak at 16.2 minutes corresponds to  $\gamma$ -mangostin ( $M+H = 397.2$ ), though this was not confirmed due to the lack of a chemical standard. The additional peaks in the mass spectrum at 11.8, 19.1, and 25.6 minutes had fragmentation patterns similar to the other xanthenes but were not investigated further.

When assessed for CYP inhibition potential, the aqueous mangosteen extract showed potent inhibition of CYP2C8 and CYP2C9 (Figure 3). CYP2C19 was also inhibited, albeit to a lesser extent. The observed  $IC_{50}$  values for CYP2C8 and CYP2C9 in human liver microsomes were 0.19 g/mL and 0.84 g/mL, respectively. CYP1A2, CYP2B6 and CYP3A4 were inhibited to lesser extents and  $IC_{50}$  values were not calculated due to incomplete inhibition curves. No measurable inhibition was observed for CYP2D6 or CYP2E1.

To further characterize the individual xanthenes found in mangosteen, qualitative reaction phenotyping experiments were carried out in recombinant

DMD 28043

CYP enzymes in order to determine the CYP isoforms responsible for their metabolism. Multiple CYP isoforms contributed to the metabolic clearance of the xanthone derivatives (Figure 4).  $\alpha$ -Mangostin, 8-desoxygartanin and 9-hydroxycalabaxanthone were primarily metabolized by CYP1A2. CYP2C9 was the major isoform responsible for the metabolism of  $\beta$ -mangostin (with minor contributions from CYP2B6, CYP2C19, CYP3A4 and CYP2D6). Gartanin appeared to be metabolized by multiple CYP isoforms as well, including CYP1A2, CYP2B6 and CYP2D6. CYP3A4 appeared to be the only isoform to metabolize 3-isomangostin to any appreciable extent.

In order to assess the CYP inhibition potential of the xanthone derivatives, a full set of  $IC_{50}$  values was obtained for each of the compounds against CYP1A2, CYP2B6, CYP2C8, CYP2C9, CYP2C19, CYP2D6, CYP2E1 and CYP3A4. For CYP3A4, both midazolam and testosterone were used as probe substrates, due to the possibility of differential drug interaction profiles between the two probes (Tucker et al., 2001; Bjornsson, 2003; Galetin et al., 2005). In addition, no more than 15 – 20% turnover of the xanthone derivatives occurred over 30 minutes in human liver microsomes. In general, the most potent inhibition was observed for the CYP2C family of enzymes. While 9-hydroxycalabaxanthone did not appear to be a potent inhibitor of CYP2C8, CYP2C9, or CYP2C19, the  $IC_{50}$  values for the other five xanthenes ranged from 0.48  $\mu$ M to 8.39  $\mu$ M against the three CYP2C isoforms (Table 1).  $IC_{50}$  values for the six compounds against the other CYP isoforms were varied and ranged from potent inhibition (8-desoxygartanin and 9-hydroxycalabaxanthone against CYP1A2) to no inhibition ( $IC_{50} > 20 \mu$ M).



DMD 28043

CYP2E1 was the only isoform for which none of the xanthone derivatives exhibited any measurable inhibition. The ability of the xanthone derivatives to inhibit CYP reductase was also examined, due to the broad inhibition profiles of the compounds. No inhibition of CYP reductase activity was observed (data not shown).

For those compounds whose  $IC_{50}$  value was less than 3  $\mu$ M, a  $K_i$  value was obtained. Five inhibitor concentrations were tested against four probe substrate concentrations. The mode of CYP inhibition (i.e., competitive or linear-mixed) was determined by visual inspection of the Dixon ( $[I]$  vs  $1/v$ ) and Lineweaver-Burke ( $1/[S]$  vs  $1/v$ ) plots (individual graphs not shown). As was observed for the  $IC_{50}$  determinations, the lowest  $K_i$  values were obtained for CYP2C8 and CYP2C9 (Table 2). All the xanthone derivatives inhibited the CYP2C isoforms in a competitive manner. Inhibition of CYP2B6 by  $\alpha$ -mangostin and gartanin was also fit to a competitive model, while inhibition of CYP1A2 by gartanin, 8-desoxygartanin and 9-hydroxycalabaxanthone appeared to conform to a linear-mixed inhibition model. Inhibition of CYP3A4 catalyzed 6 $\beta$ -hydroxytestosterone formation by  $\alpha$ -mangostin and 9-desoxygartanin was competitive while inhibition of the same isoform by 3-isomangostin was fit to a linear-mixed model.

The ability of each of the six xanthone analogs to inhibit CYP activity in a time-dependent fashion was examined against CYP1A2, CYP2B6, CYP2C8, CYP2C9, CYP2C19, CYP2D6 and CYP3A4 in pooled human liver microsomes. Relatively weak time-dependent inhibition of CYP1A2 was observed for  $\alpha$ -

DMD 28043

mangostin and 3-isomangostin (data not shown). The addition of glutathione to the incubations attenuated the time-dependent inhibition of CYP1A2 by the two xanthone compounds. No other time-dependent inhibition of CYP activity was observed.

Finally, estimated plasma concentrations of  $\alpha$ -mangostin following various doses of mangosteen were obtained using SimCYP and compared to the *in vitro*  $K_i$  values for each CYP isoform.  $\alpha$ -Mangostin was chosen because it was the most abundant xanthone identified in the aqueous extracts of mangosteen. Two doses of mangosteen were modeled, a low dose of 6.5 mg bid and a higher dose of 75 mg bid. The doses represent a range of either measured or labeled  $\alpha$ -mangostin concentrations from multiple mangosteen products. In addition, to account for a range of absorption characteristics that may arise from different mangosteen products or formulations, predicted plasma concentrations were also plotted for various  $f_a$  values for the 75 mg dose. The predicted  $C_{max}$  value following the 75 mg bid dose ( $f_a = 1$ ) was 0.881 mg/L (2.15  $\mu$ M), which is approximately 3.36-fold and 3.58-fold higher than the observed *in vitro*  $K_i$  values for CYP2C8 and CYP2C9, respectively (Figure 5). The  $C_{max}$  values for the 75 mg dose at  $f_a = 0.75$  and  $f_a = 0.5$  were also observed to be above the *in vitro*  $K_i$  values. As no accumulation was observed, only the plasma concentrations following the first dose of mangosteen are shown. In SimCYP drug interaction simulations using rosiglitazone as a model substrate for CYP2C8 and CYP2C9, the median ratio of AUC values in the presence of  $\alpha$ -mangostin compared to

DMD 28043

control simulations ( $AUC_i/AUC$ ) ranged from 2.11 for the 6.5 mg dose up to 11.68 for the 75 mg dose ( $f_a = 1$ ).

DMD 28043

## DISCUSSION

The use of herbal-based and nontraditional remedies has increased significantly over the past decade (Craig, 1999; Ritchie, 2007). In many cases herbal remedies are commonly combined with prescription drugs. Often these herbal supplements are not subject to rigorous safety testing and as such have not been fully assessed for quantities of active ingredients or potential safety issues. Not surprisingly, the number of reported cases of herbal-drug interactions has also increased (Foti and Wahlstrom, 2008). In an attempt to partially address the issue, the U.S. Food and Drug Administration (FDA) has recently issued a guidance document pertaining to efficacy and safety claims surrounding an herbal or nutritional supplement (<http://www.cfsan.fda.gov/~dms/dsclmgu2.html>).

A number of structural classes known to cause CYP inhibition such as alkaloids, flavones and polyphenols have been identified in herbal products (Foti and Wahlstrom, 2008). Structurally, the xanthenes found in mangosteen also appear to be good ligands for CYP enzymes as evidenced by the broad spectrum of CYP-catalyzed metabolism, nonselective inhibition of multiple CYP isoforms and their previously noted interactions with CYP19 (aromatase). The xanthenes found in mangosteen have multiple phenolic groups which may contribute to both their efficacious and inhibitory effects. Phenol containing compounds such as the flavanol quercetin have been shown to be potent competitive inhibitors of CYP2C9 by occupying the flurbiprofen binding site of CYP2C9 (Si et al., 2008). The polyphenolic substructures of the xanthenes

DMD 28043

found in mangosteen may suggest a similar mechanism of inhibition for these compounds. Interestingly, two of the xanthenes,  $\alpha$ -mangostin and 3-isomangostin, were capable of competitively inhibiting CYP2C8 and CYP2C9 activity while not appearing to undergo significant metabolism by these isoforms.

Xanthone containing remedies such as mangosteen have been used throughout the years as treatments for numerous ailments. Current therapeutic claims for xanthenes range from maintaining healthy immune, respiratory and gastrointestinal function to lowering blood pressure and decreasing allergic sensitivities. Mangosteen components have been shown to inhibit prostaglandin E2 and lipopolysaccharide-induced cyclooxygenase-2 expression in response to inflammation, have anti-proliferative and apoptotic effects on breast cancer cell lines and inhibit HIV-1 protease activity *in vitro* (Nakatani et al., 2002; Nakatani et al., 2004; Moongkarndi et al., 2004; Chen et al., 1996). It has also been proposed that xanthenes like those found in the mangosteen fruit may aid in slowing the progress of neurodegenerative diseases such as Alzheimer's disease, Parkinson's disease and amyotrophic lateral sclerosis (Di Matteo and Esposito, 2003). Many of these therapeutic benefits are thought to stem from their ability to effectively scavenge reactive oxygen species. More recently, fused-xanthone derivatives such as furanoxanthone and pyranoxanthone have been noted for their anti-tumor activity (Pouli and Marakos, 2009).

While the therapeutic benefits of xanthone-based remedies may certainly exist, the potential also exists for safety risks to arise when the herbal remedy is co-administered with prescription drugs. Drugs such as warfarin (anti-coagulant),

DMD 28043

piroxicam and celecoxib (arthritis/pain), baclofen, valproic acid and phenytoin (Parkinson's), paclitaxel (anti-tumor) and omeprazole (gastrointestinal) are among the most commonly prescribed medications in the U.S (<http://www.bcbstx.com/pdf/druglist.pdf>) and are all substrates for the CYP2C family of enzymes (Rendic, 2002). More importantly, warfarin, valproic acid, phenytoin and paclitaxel have all been classified as “narrow therapeutic index” drugs (Bollag et al., 1995; Burns, 1999; Shakya et al., 2008). Inhibiting the metabolism of these drugs in any manner could result in toxicological consequences. Omeprazole has been classified by the FDA as a “sensitive” CYP2C19 substrate, or one whose plasma AUC values may increase in excess of 5-fold in the presence of a CYP inhibitor (US Food and Drug Administration, 2006). It is possible to envision mangosteen being consumed in combination with these drugs due to the similar patient populations that may benefit from the use of mangosteen or one of the prescription drugs mentioned above. When the potent inhibition of CYP2C8, CYP2C9 and CYP2C19 by the xanthone derivatives is taken into account, plasma concentrations of the prescription drugs may rise to potentially dangerous levels.

The ability to predict *in vivo* exposure levels of a given drug (or inhibitor) using modeling and simulation programs such as SimCYP is a useful tool in the design of drug efficacy and safety studies (Rostami-Hodjegan and Tucker, 2007). The FDA guidance on drug interactions advises that the potential of an *in vivo* drug interaction occurring becomes likely if an interaction is observed *in vitro* and if  $[I] / K_i > 1$ , where  $[I]$  is the mean steady-state  $C_{max}$  value and  $K_i$  is the inhibition

DMD 28043

constant. Using SimCYP, the  $C_{\max}$  value of  $\alpha$ -mangostin following a 75 mg dose of mangosteen was predicted to be 2.15  $\mu$ M (0.881 mg/L; Figure 5). When compared to their respective  $K_i$  values as determined *in vitro*,  $[I] / K_i$  is equal to 3.36 and 3.58 for CYP2C8 and CYP2C9, respectively. While this is not conclusive evidence of a clinically relevant drug interaction, in light of the additional confirmation afforded by the drug interaction simulation, it would be cause for additional investigation if the inhibitor were a prescription therapeutic.

Furthermore, the inhibition of CYP activity by aqueous extracts of mangosteen pericarp *in vitro* is important in light of the prevalent *in vitro* – *in vivo* disconnect for CYP-mediated herbal – drug interactions. A proposed reason for this observed disconnect are the extraction techniques and solvents used *in vitro* that may not accurately reflect the solubility and absorption characteristics of the herbal components *in vivo* (Gurley, et al., 2005b). Additional discrepancies in the *in vitro* and *in vivo* drug interaction potentials may also be due to the numerous formulations that are available for a given herbal supplement. It can be postulated that herbal extractions in a purely aqueous environment may be more indicative of the *in vivo* scenario.

In conclusion, the individual xanthone components of the mangosteen fruit have been shown to be both substrates and inhibitors of multiple CYP isoforms. While the therapeutic benefits of mangosteen are still being investigated, the pending safety profile of the herbal remedy cannot be ignored. Further studies are required to determine whether or not consumption of mangosteen in combination with prescription medication may result in a drug interaction *in vivo*.

DMD 28043

Until such data becomes available, patients taking traditional medication should exercise caution when using xanthone containing supplements such as mangosteen.



DMD 28043

## References

Balunas MJ, Su B, Brueggemeier RW and Kinghom AD (2008) Xanthonenes from the botanical dietary supplement mangosteen (*Garcinia mangostana*) with aromatase inhibitory activity. *J Nat Prod* **71**: 1161-1166.

Bjornsson TD, Callaghan JT, Einolf HJ, Fischer V, Gan L, Grimm S, Kao J, King SP, Miwa G, Ni L, Kumar G, McLeod J, Obach RS, Roberts S, Roe A, Shah A, Snikeris F, Sullivan JT, Tweedie D, Vega JM, Walsh J and Wrighton SA (2003) The conduct of *in vitro* and *in vivo* drug-drug interaction studies: A Pharmaceutical Research and Manufacturers of America (PhRMA) perspective. *Drug Metab Dispos* **31**: 815-832.

Blumenthal M, Ferrier GKL and Cavaliere C (2006) Total sales of herbal supplements in the United States show steady growth. *HerbalGram* **71**:64-66

Bollag DM, McQueney PA, Zhu J, Hensens O, Koupal L, Liesch J, Goetz M, Lazarides E and Woods CM (1995) Epothilones, a new class of microtubule-stabilizing agents with a taxol-like mechanism of action. *Cancer Res* **55**:2325-2333)

Burns M (1999) Management of narrow therapeutic index drugs. *J Thromb Thrombolysis* **7**:137-143.

DMD 28043

Chang TK, Chen J and Benetton SA (2002) *In vitro* effect of standardized ginseng extracts and individual ginsenosides on the catalytic activity of human CYP1A1, CYP1A2, and CYP1B1. *Drug Metab Dispos* **30**: 378-384.

Chen SX, Wan M and Loh BN (1996) Active constituents against HIV-1 protease from *Garcinia mangostana*. *Planta Med* **62**: 381-382.

Craig WJ (1999) Health promoting properties of common herbs. *Am J Clin Nutr* **70**:491S-499S.

Di Matteo V and Esposito E (2003) Biochemical and therapeutic effects of antioxidants in the treatment of Alzheimer's disease, Parkinson's disease and amyotrophic lateral sclerosis. *Curr Drug Targets CNS Neurol Disord* **2**: 95-107.

Foster BC, Foster MS, Vandenhoeck S, Krantis A, Budzinski JW, Arnason JT, Gallicano KD and Choudri S (2001) An *in vitro* evaluation of human cytochrome P450 3A4 and P-glycoprotein inhibition by garlic. *J Pharm Pharm Sci* **4**: 176-184.

Foti RS and Wahlstrom JL (2008) The role of dietary supplements in cytochrome P450 –mediated drug interactions. *Lat Am Bull Carib Med Arom Plants* **7**: 66-84.

DMD 28043

Galetin A, Ito K, Hallifax D and Houston JB (2005) CYP3A4 substrate selection and substitution in the prediction of potential drug-drug interactions. *J Pharmacol Exp Ther* **314**:180-190.

Gurley BJ, Gardner SF, Hubbard MA, Williams DK, Gentry WB, Cui Y and Ang CY (2005a) Clinical assessment of effects of botanical supplementation on cytochrome P450 phenotypes in the elderly: St John's wort, garlic oil, Panax ginseng and Ginkgo biloba. *Drugs Aging* **22**: 522-539.

Gurley BJ, Gardner SF, Hubbard MA, Williams DK, Gentry WB, Khan IA and Shah A (2005b) *In vivo* effects of goldenseal, kava kava, black cohosh, and valerian on human cytochrome P450 1A2, 2D6, 2E1, and 3A4/5 phenotypes. *Clin Pharmacol Ther* **77**: 415-26.

He N and Edeki T (2004) The inhibitory effects of herbal components on CYP2C9 and CYP3A4 catalytic activities in human liver microsomes. *Am J Ther* **11**: 206-212.

Ji X, Avula B and Khan IA (2007) Quantitative and qualitative determination of six xanthenes in *Garcinia mangostana* L. by LC-PDA and LC-ESI-MS. *J Pharm Biomed Anal* **43**: 1270-1276.

DMD 28043

Jung HA, Su BN, Keller WJ, Mehta RG and Kinghom AD (2006) Antioxidant xanthenes from the pericarp of *Garcinia mangostana* (Mangosteen). *J Agric Food Chem* **54**: 2077-2082.

Kosem N, Youn-Hee H and Moongkarndi P (2007) Antioxidant and cytoprotective activities of methanolic extract from *Garcinia mangostana* hulls. *Sci Asia* **33**: 283-292.

Liu Y, Zhang JW, Li W, Ma H, Sun J, Deng MC and Yang L (2006) Ginsenoside metabolites, rather than naturally occurring ginsenosides, lead to inhibition of human cytochrome P450 enzymes. *Toxicol Sci* **91**: 356-364.

Markowitz JS, Donovan JL, Devane CL, Taylor RM, Ruan Y, Wang JS and Chavin KD (2003) Multiple doses of saw palmetto (*Serenoa repens*) did not alter cytochrome P450 2D6 and 3A4 activity in normal volunteers. *Clin Pharmacol Ther* **74**: 536-542.

Modarai M, Gertsch J, Suter A, Heinrich M and Kortenkamp A (2007) Cytochrome P450 inhibitory action of Echinacea preparations differs widely and co-varies with alkylamide content. *J Pharm Pharmacol* **59**: 567-573.

Moongkarndi P, Kosem N, Kaslungka S, Luanratana O, Pongpan N and Neungton N (2004) Antiproliferation, antioxidation and induction of apoptosis by

DMD 28043

*Garcinia mangostana* (mangosteen) on SKBR3 human breast cancer cell line. *J Ethnopharmacol* **90**: 161-166.

Nakatani K, Nakahata N Arakawa T, Yasuda H and Ohizumi Y (2002) Inhibition of cyclooxygenase and prostaglandin E2 synthesis by gamma-mangostin, a xanthone derivative in mangosteen, in C6 rat glioma cells. *Biochem Pharmacol* **63**: 73-79.

Nakatani K, Yamajuni T, Kondo N, Arakawa T, Oosawa K, Shimura S, Inoue H and Ohizumi Y (2004) gamma-Mangostin inhibits inhibitor-kappaB kinase activity and decreases lipopolysaccharide-induced cyclooxygenase-2 gene expression in C6 rat glioma cells. *Mol Pharmacol* **66**: 667-674.

Obach RS (2000) Inhibition of human cytochrome P450 enzymes by constituents of St. John's Wort, an herbal preparation used in the treatment of depression. *J Pharmacol Exp Ther* **294**: 88-95.

Pouli N and Marakos P (2009) Fused xanthone derivatives as antiproliferative agents. *Anticancer Agents Med Chem* **9**: 77-98.

Rendic S (2002) Summary of information on human CYP enzymes: Human P450 metabolism data. *Drug Metab Rev* **34**:83-448.

DMD 28043

Ritchie MR (2007) Use of herbal supplements and nutritional supplements in the UK: what do we know about their pattern of usage? *Proc Nutr Soc* **66**:479-482.

Rostami-Hodjegan A and Tucker GT (2007) Simulation and prediction of in vivo drug metabolism in human populations from in vitro data. *Nature Rev* **6**:140-149.

Shakya G, Malla S, Shakya KN and Shrestha R (2008) Therapeutic drug monitoring of antiepileptic drugs. *J Nepal Med Assoc* **47**:94-97.

Si D, Wang Y, Guo Y, Wang J and Zhou H (2008) Mechanism of CYP2C9 inhibition by flavones and flavanols. *Drug Metab Dispos* **Fast Forward**:DMD#23416.

Skalli S, Zaid A and Soulaymani R (2007) Drug interactions with herbal medicines. *Ther Drug Monit* **29**:679-686.

Tirona RG and Bailey DG (2006) Herbal product-drug interactions mediated by induction. *Br J Clin Pharmacol* **61**:677-681.

Tucker GT, Houston JB and Huang SM (2001) EUFEPS conference report. Optimising drug development: strategies to assess drug metabolism/transporter interaction potential – towards a consensus. European Federation of Pharmaceutical Sciences. *Eur J Pharm Sci* **13**: 417-428.

DMD 28043

U.S. Food and Drug Administration (2006) Guidance for industry: Drug interaction studies – Study design, data analysis and implications for dosing, and labeling. Available at <http://www.fda.gov/cder/guidance/6695dft.pdf>.

Walsky RL and Obach RS (2004) Validated assays for human cytochrome P450 activities. *Drug Metab Dispos* **32**: 647-660.

Yale SH and Glurich I (2005) Analysis of the inhibitory potential of Ginkgo biloba, Echinacea purpurea, and Serenoa repens on the metabolic activity of cytochrome P450 3A4, 2D6, and 2C9. *J Altern Complement Med* **11**: 433-439.

DMD 28043

### *Figure Legends*

Figure 1. Structures of xanthone derivatives found in mangosteen.

Figure 2. Representative chromatogram of xanthenes found in the aqueous extract of mangosteen. A similar pattern was observed for the acetone extract.

Figure 3. Inhibition of CYP2C8, CYP2C9 and CYP2C19 by the aqueous mangosteen extract.

Figure 4. Percent parent compound remaining for each of the six xanthone derivatives in recombinant CYP enzymes following a 30 minute incubation with NADPH.

Figure 5. Estimated plasma concentrations of  $\alpha$ -mangostin following recommended doses of mangosteen extract. Dose levels represent a range of  $\alpha$ -mangostin found in a single dose of mangosteen extract.



DMD 28043

Table 1.  $IC_{50}$  values in human liver microsomes for the individual xanthone derivatives (Abbreviations:  $\alpha$ -mang,  $\alpha$ -mangostin;  $\beta$ -mang,  $\beta$ -mangostin; 3-iso, 3-isomangostin; 8-desoxy, 8-desoxygartanin; 9-hydroxy, 9-hydroxycalabaxanthone). CYP3A4-M and CYP3A4-T refer to the use of midazolam or testosterone as probe substrates for CYP3A4, respectively.

	<b><math>IC_{50}</math> Values in Human Liver Microsomes (<math>\mu</math>M)</b>					
	<b><math>\alpha</math>-mang</b>	<b><math>\beta</math>-mang</b>	<b>gartanin</b>	<b>3-iso</b>	<b>8-desoxy</b>	<b>9-hydroxy</b>
CYP1A2	> 20	5.99	1.13	5.94	0.57	0.50
CYP2B6	2.89	10.6	1.60	5.23	> 20	> 20
CYP2C8	0.88	8.39	6.28	0.64	1.85	14.1
CYP2C9	1.14	0.77	4.66	0.48	3.80	17.6
CYP2C19	4.54	4.45	4.75	3.99	3.41	9.18
CYP2D6	7.36	> 20	> 20	6.00	10.7	> 20
CYP2E1	> 20	> 20	> 20	> 20	> 20	> 20
CYP3A4-M	7.98	> 20	7.89	5.65	8.18	> 20
CYP3A4-T	2.49	6.39	4.94	2.23	1.75	> 20

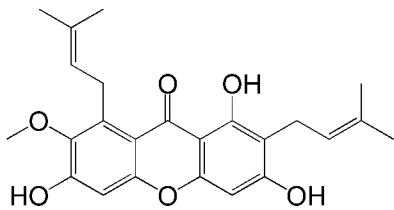
DMD 28043

Table 2.  $K_i$  values for the individual xanthone derivatives in human liver microsomes (Abbreviations:  $\alpha$ -mang,  $\alpha$ -mangostin;  $\beta$ -mang,  $\beta$ -mangostin; 3-iso, 3-isomangostin; 8-desoxy, 8-desoxygartanin; 9-hydroxy, 9-hydroxycalabaxanthone). (C) indicates that the inhibition data was fit to a competitive model while (M) indicates a linear-mixed model.

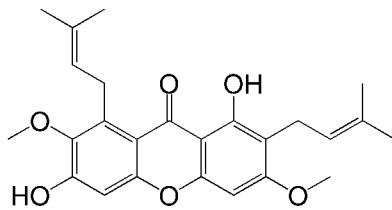
	<b><math>K_i</math> Values in Human Liver Microsomes (<math>\mu</math>M)</b>					
	<b><math>\alpha</math>-mang</b>	<b><math>\beta</math>-mang</b>	<b>gartanin</b>	<b>3-iso</b>	<b>8-desoxy</b>	<b>9-hydroxy</b>
CYP1A2	---	---	3.58 (M)	---	3.19 (M)	2.63 (M)
CYP2B6	1.91 (C)	---	1.01 (C)	---	---	---
CYP2C8	0.64 (C)	---	---	0.66 (C)	2.80 (C)	---
CYP2C9	0.60 (C)	0.34 (C)	---	0.40 (C)	---	---
CYP2C19	---	---	---	---	---	---
CYP2D6	---	---	---	---	---	---
CYP2E1	---	---	---	---	---	---
CYP3A4-M	---	---	---	---	---	---
CYP3A4-T	2.79 (C)	---	---	3.23 (M)	1.41 (C)	---

(C) = competitive; (M) = linear mixed

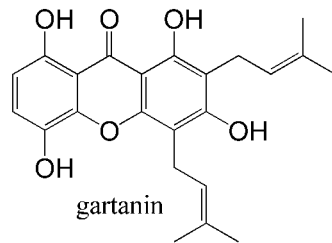
Figure 1



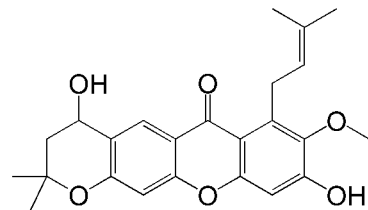
$\alpha$ -mangostin



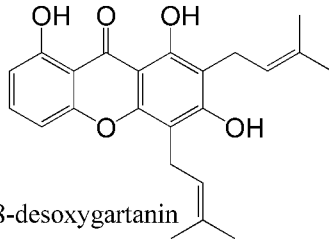
$\beta$ -mangostin



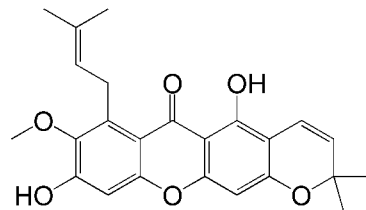
gartanin



3-isomangostin



8-desoxygartanin



9-hydroxycalabaxanthone

**Figure 2**

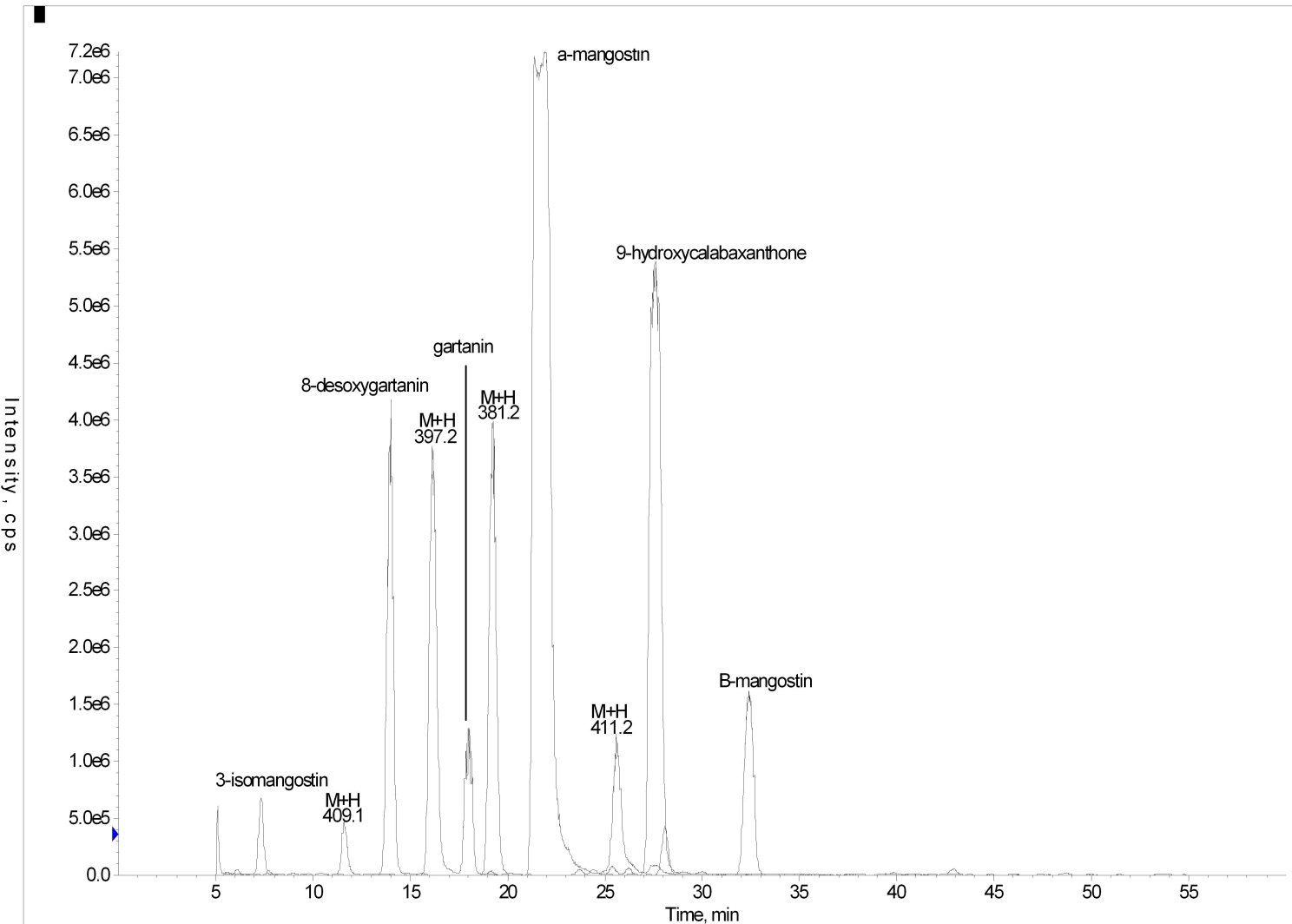


Figure 3

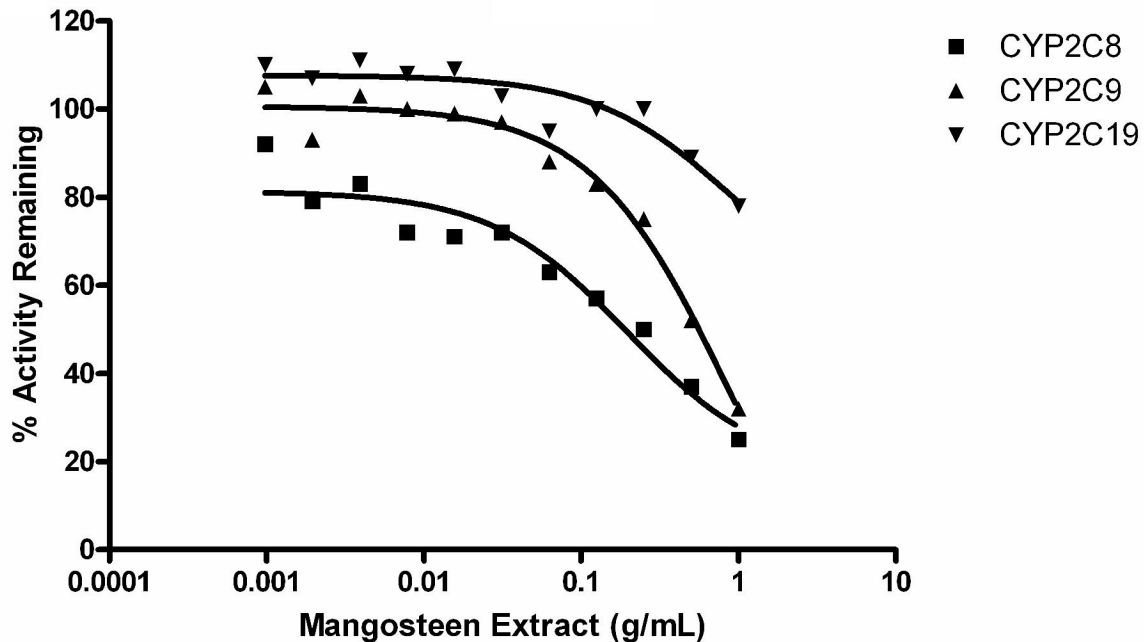


Figure 4

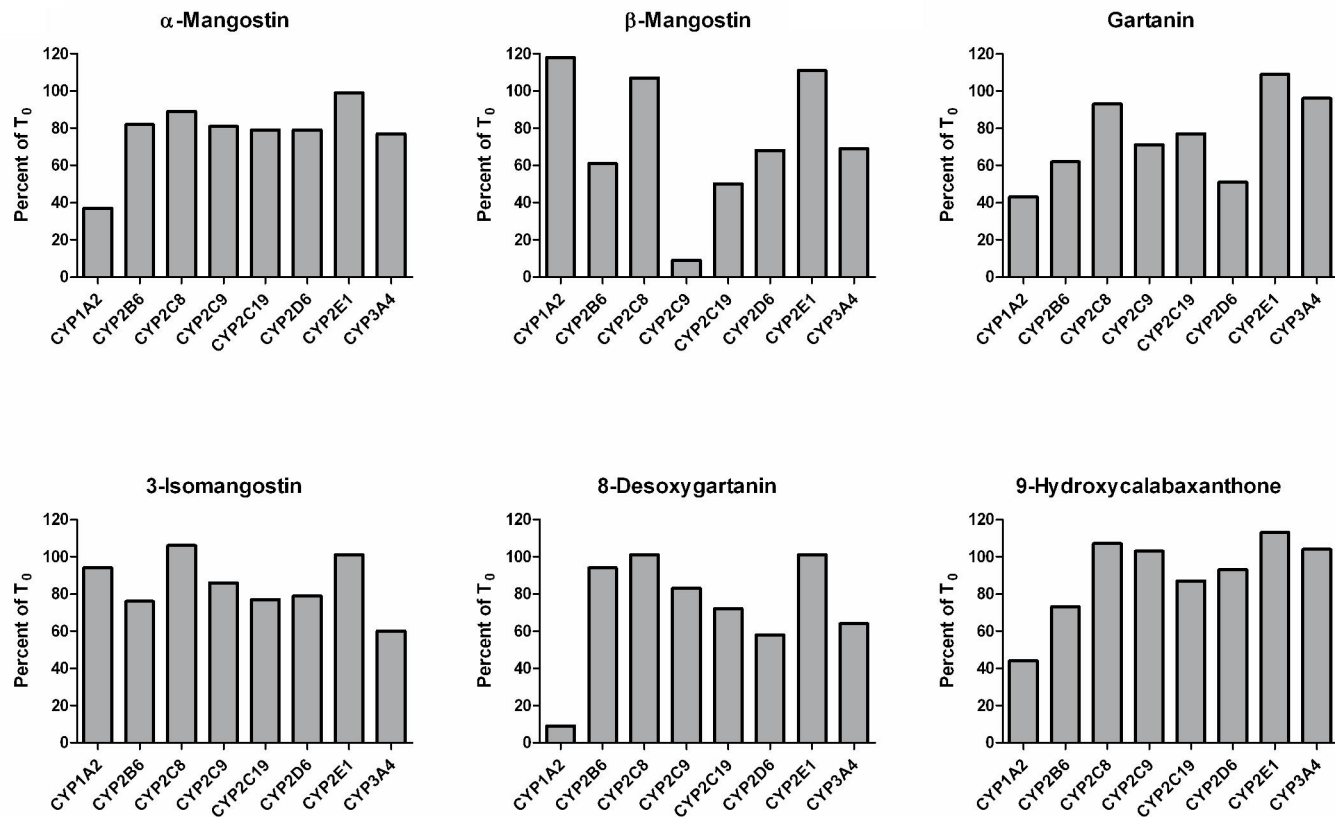


Figure 5

